

Weak Signal Inclusion Under Dependence and Applications in Genome-wide Association Study *

X. Jessie Jeng, Yifei Hu, Quan Sun and Yun Li

December 29, 2022

Abstract

Motivated by the inquiries of weak signals in underpowered genome-wide association studies (GWASs), we consider the problem of retaining true signals that are not strong enough to be individually separable from a large amount of noise. We address the challenge from the perspective of false negative control and present false negative control (FNC) screening, a data-driven method to efficiently regulate false negative proportion at a user-specified level. FNC screening is developed in a realistic setting with arbitrary covariance dependence between variables. We calibrate the overall dependence through a parameter whose scale is compatible with the existing phase diagram in high-dimensional sparse inference. Utilizing the new calibration, we asymptotically explicate the joint effect of covariance dependence, signal sparsity, and signal intensity on the proposed method. We interpret the results using a new phase diagram, which shows that FNC screening can efficiently select a set of candidate variables to retain a high proportion of signals even when the signals are not individually separable from noise. Finite sample performance of FNC screening is compared to those of several existing methods in simulation studies. The proposed method outperforms the others in

*Address for correspondence: X. Jessie Jeng, Department of Statistics, North Carolina State University, SAS Hall, 2311 Stinson Dr., Raleigh, NC 27695-8203, USA. E-mail: xjjeng@ncsu.edu.

adapting to a user-specified false negative control level. We implement FNC screening to empower a two-stage GWAS procedure, which demonstrates substantial power gain when working with limited sample sizes in real applications.

Keywords: Arbitrary Covariance Dependence; False Negative Control; Underpowered GWAS; High-Dimensional Data; User Adaptive Method

1 Introduction

Since established in early 2000s, genome-wide association studies (GWASs) have been very successful in identifying genetic variants predisposing to complex traits and diseases, often by accumulating very large sample sizes (Hu et al., 2021; Mikhaylova et al., 2021; Zhao et al., 2022; Mahajan et al., 2022). Yet, GWAS of many diseases remain underpowered, especially for non-European ancestries (Sun et al., 2022; Liu et al., 2022). It has come to be understood that the bulk of the missing heritability can be attributed to a large number of common variants with small effect sizes. Such weak signals have not been sufficiently addressed by statistical methods.

Over the years, important contributions have been made towards two related problems in high-dimensional statistical inference. One is the detection of mixture models, which addresses the problem of “detecting” the existence of sparse signals without specifying their exact locations (see, e.g. Donoho and Jin (2004), Arias-Castro et al. (2011), Cai et al. (2011)). The second is the separation of signals from noise variables, for which multiple testing has been used to control inflated false positive errors under high-dimensionality. Figure 1 modified from Cai and Sun (2017a) illustrates the theoretical demarcation on the difficulty levels of these two problems in the setting where all variables are independent. Given a sparsity level, signal intensity needs to be large enough (above the undetectable region) for the signals to be detectable by a global testing procedure. For the signals to be well-separated from noise variables with negligible classification errors, signal intensity needs to be even larger (entering the classifiable region). Detailed interpretations for the classifiable boundary can be found in Arias-Castro and Chen (2017). Finer allocations of

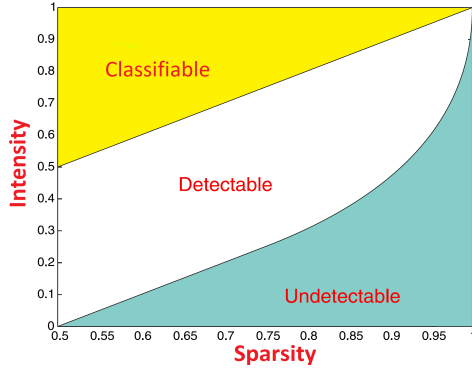


Figure 1: Phase diagram for signal detection and classification. Signals in the middle region are only detectable for their existence but cannot be well-separated from noise.

signals in the classifiable region corresponding to different forms of classification errors are summarized in [Gao and Stoev \(2021\)](#). Other versions of [Figure 1](#) and related analyses under different model settings include but not limited to [Donoho and Jin \(2004\)](#), [Donoho and Jin \(2015\)](#), [Ji and Jin \(2012\)](#), [Ji and Zhao \(2014\)](#), [Jin et al. \(2017\)](#), [Chen et al. \(2019\)](#), etc.

In this paper, we focus on signals in the middle white region of [Figure 1](#), which can only be detected for their existence by global testing but are not separable from noise by multiple testing. Such weak signals commonly exist in large-scale data analysis and play vital roles in biomedical applications. In GWAS, such signals can be the common genetic variants that have small effect sizes and account for a large fraction of the missing heritability. Despite its importance, how to effectively retain detectable yet unclassifiable signals raises a bottleneck challenge in high-dimensional sparse inference. New developments are needed to bridge the methodological gap.

To retain weak signals in the middle region of [Figure 1](#), we consider strategies to effectively control false negative errors. In the literature, study of false negative control largely lags behind. One cannot simply switch the null and alternative hypotheses and achieve false negative control by a hypothesis testing approach because, unlike the null distribution, alternative distributions are often unknown and hard to estimate from the data. Moreover, the targeted control level of false negatives cannot be achieved by manipulating the nominal level of a multiple testing procedure because the exact trade-off relationship between false negative and false positive errors depends on the signal-to-noise ratio, which is unknown in

real applications.

We propose False Negative Control (FNC) screening, a data-driven method to effectively control the false negative proportion ($\text{FNP} = \text{number of false negatives} / \text{number of true signals}$) at a user-specified level. The measure of FNP can be interpreted as the empirical Type II error of a selection rule. We have found that, in different application scenarios, researchers often have different tolerance levels for false negative errors. Our procedure controls FNP at a user-specified level under conditions weak enough to allow for unclassifiable signals. Moreover, its adaptivity to a given FNP level, such as 0.1, allows the procedure to exclude a certain amount of the weakest signals to reduce possibly a large number of false positives. Note that the FNP measure is different from the measure of false non-discovery rate, which is defined as the expected value of the proportion of false negatives among the accepted null hypotheses for a single-step multiple testing procedure (Genovese and Wasserman, 2002; Sarkar, 2006).

In the literature, false negative control methods have only appeared recently. For example, the AFNC method in Jeng et al. (2016) was proposed to control the so-called signal missing rate to detect rare variants in next-generation sequencing data analysis. The MDR method in Cai and Sun (2017b) uses an empirical Bayesian approach to control the mean value of FNP. Both AFNC and MDR were developed assuming independent variables. False negative control under specific dependence settings has been considered in Jeng et al. (2019), where the AdSMR method was developed to control signal missing rate under block dependence. The FNC-Reg approach in Jeng and Chen (2019) considers FNP control in linear regression under specific conditions on variable dependence and signal sparsity to facilitate accurate precision matrix estimation and bias mitigation in linear regression.

In this paper, we develop FNC screening in a realistic setting with arbitrary covariance dependence between variables. We propose to calibrate the overall dependence strength through a parameter whose scale is compatible with the parameter space of the phase diagram presented in Figure 1. Utilizing the new calibration, we are able to asymptotically explicate the joint effect of covariance dependence, signal sparsity, and signal intensity on the proposed method. We interpret the results using a new phase diagram, which shows the power gain

of the new method in retaining weak signals.

Finite sample performance of FNC screening is studied in simulation examples where the data are generated under several commonly observed dependence structures. These dependence structures range from weak to strong in our dependence calibration system. The new method outperforms existing methods in adapting to a user-specified FNP control level.

We apply FNC screening to empower a standard two-stage procedure in GWAS. The empowered procedure is tested and benchmarked against a classical GWAS procedure in 145 working datasets from UK Biobank, each with a sample size $n = 5000$. It shows that the empowered procedure can substantially increase power of signal discovery while adopting the same control level on family-wise error rate. The results are further evaluated using a large validation dataset with 500,000 samples. It shows that most of the genetic variants selected by the empowered procedure have very small validation p-values and are likely to be true signals. We expect the empowered procedure to be useful in alleviating critical issues in underpowered GWASs for rare diseases and minority populations.

2 Method and Theory

We consider a two-groups model with continuous null distribution F_0 . Suppose that the observed test statistics

$$X_j \sim F_0 \cdot 1\{j \in I_0\} + F_j \cdot 1\{j \in I_1\}, \quad j = 1, \dots, m, \quad (1)$$

where I_0 is the set of indices for noise variables, I_1 is the set of indices for signal variables, and F_j are the signal distributions. All I_0 , I_1 , and F_j are unknown. One can perform inverse normal transformation as $Z_j = \Phi^{-1}(F_0(X_j))$, where Φ^{-1} is the inverse of the standard normal cumulative distribution. Then, we have

$$Z_j \sim \Phi \cdot 1\{j \in I_0\} + G_j \cdot 1\{j \in I_1\}, \quad j = 1, \dots, m, \quad (2)$$

where G_j are the unknown signal distributions after the transformation. For presentation simplicity, we assume that $G_j(t) < \Phi(t)$ for all $t \in \mathbb{R}$. i.e., signal variables tend to show larger values than noise variables. This assumption can be easily generalized to signals with two-sided effects.

2.1 False negative control screening

Consider a selection rule with threshold t . Define the numbers of selected variables, false positives, and false negatives as

$$R(t) = \sum_{j=1}^m 1_{\{Z_j > t\}}, \quad FP(t) = \sum_{j \in I_0} 1_{\{Z_j > t\}}, \quad FN(t) = \sum_{j \in I_1} 1_{\{Z_j \leq t\}}.$$

The above quantities and other classification measurements including the numbers of true positives (TP) and true negatives (TN) are summarized in [Table 1](#).

Table 1: Classification matrix of the selection rule with threshold t .

	Not Selected	Selected	Total
Negative	TN(t)	FP(t)	$m - s$
Positive	FN(t)	TP(t)	s
Total	$m - R(t)$	$R(t)$	m

Note that $R(t)$ and m can be directly observed. $FP(t)$, $FN(t)$, $TP(t)$, $TN(t)$, and $s(= |I_1|)$ are unknown because I_0 and I_1 are unknown. A generalization to two-sided signal effects can be accommodated by replacing Z_j with $|Z_j|$ and only allowing $t > 0$.

Next, define FNP with respect to t as

$$FNP(t) = FN(t)/s. \tag{3}$$

$FNP(t)$ may be regarded as the empirical type II error that is non-decreasing with respect to t . We aim to determine a selection threshold \hat{t} such that the corresponding $FNP(\hat{t})$ can be controlled at a desirable low level.

Our new method is based on the approximation of $FNP(t)$ for a given t . Utilizing the

fact that $s = \text{FN}(t) + \text{TP}(t)$ and $\text{R}(t) = \text{FP}(t) + \text{TP}(t)$ as shown in Table 1, we have

$$\text{FNP}(t) = \text{FN}(t)/s = 1 - (\text{R}(t) - \text{FP}(t))/s, \quad (4)$$

where $\text{R}(t)$ is directly observable from the data. Because the noise distribution of Z_j is $N(0, 1)$ and there are $m - s$ noise variables, $\text{FP}(t)$ can be approximated by its mean value $E(\text{FP}(t)) = (m - s)\bar{\Phi}(t)$, where $\bar{\Phi}(t) = 1 - \Phi(t)$. For illustration purpose, we first assume that the true value of s is known and define

$$\widehat{\text{FNP}}(t) = \max\{1 - \text{R}(t)/s + (m - s)\bar{\Phi}(t)/s, 0\}. \quad (5)$$

$\widehat{\text{FNP}}(t)$ with an estimated s will be discussed in Section 2.3. Note that $\widehat{\text{FNP}}(t)$ is not the mean value of $\text{FNP}(t)$, and its construction does not require information of the signal distributions $G_j, j \in I_1$. If two-sided signal effects are under consideration, we can simply modify $\widehat{\text{FNP}}(t)$ by replacing $(m - s)$ with $2(m - s)$.

Now given a user-specified control level, $\beta(> 0)$, on FNP, we determine the selection threshold as

$$\hat{t}(\beta) = \sup \{t : \widehat{\text{FNP}}(t) < \beta\}, \quad (6)$$

and select all the candidates with $Z_j > \hat{t}(\beta)$. If two-sided signal effects are considered, all candidates with $|Z_j| > \hat{t}(\beta)$ will be selected. We refer to this procedure as False Negative Control (FNC) screening.

The proposed FNC screening procedure has several key features. (1) When all variables are ranked such that $Z_{(1)} \geq Z_{(2)} \geq \dots \geq Z_{(m)}$, FNC screening selects the smallest subset from the top whose estimated FNP is less than β . Such selection process can effectively retain a high proportion of true signals while excluding unnecessary noise variables. (2) FNC screening can be implemented as long as the marginal distribution of noise variables is known. The procedure does not require any information of the signal distributions nor dependence between the variables. (3) In real studies, researchers may have different tolerance levels for false negative errors. Adapting to a user-specified control level on FNP can substantially

increase the applicability of the method. (4) From a practical standpoint, allowing for a certain percentage of FNP may avoid possibly a large number of false positives as a trade off.

We would like to point out that although there exists a relationship between $\text{FNP}(t)$ and false discovery proportion ($\text{FDP}(t) = \text{FP}(t)/\text{R}(t)$) through

$$\text{FNP}(t) = 1 - \frac{\text{R}(t)}{s} + \frac{\text{FDP}(t) \cdot \text{R}(t)}{s},$$

consistent estimation of $\text{FDP}(t)$ by an estimator $\widehat{\text{FDP}}(t)$ does not imply consistent estimation of $\text{FNP}(t)$ by $1 - \text{R}(t)/s + \widehat{\text{FDP}}(t) \cdot \text{R}(t)/s$. This is because the estimation error for $\text{FNP}(t)$ also depends on the factor of $\text{R}(t)/s$, whose magnitude varies with t and can be on the order of $O(m/s)$ for $t = O(1)$.

2.2 Theoretical properties under the Gaussian assumption

In this section, we study the asymptotic behavior of the proposed FNC screening method in the setting of sparse inference where signal proportion $\pi(= s/m)$ converges to zero as $m \rightarrow \infty$. Specifically, we assume

$$\pi = \pi_m = m^{-\gamma}, \quad \gamma \in (0, 1). \quad (7)$$

Consequently, the number of signals $s(= m^{1-\gamma})$ increases with m but of a smaller order. Such calibration on sparsity has been widely adopted in literature, see e.g. [Donoho and Jin \(2004\)](#), [Cai et al. \(2011\)](#), [Arias-Castro et al. \(2011\)](#), [Ji and Jin \(2012\)](#), [Ji and Zhao \(2014\)](#), [Jin et al. \(2017\)](#).

In this section, we explicate the combined effects of signal sparsity, signal intensity, and dependence between variables under the assumption that

$$(Z_1, \dots, Z_m) \sim N_m(\mu, \Sigma), \quad (8)$$

where μ is a m -dimensional vector with $\mu_j = A_j \cdot 1\{j \in I_1\}$, $A_j > 0$, and Σ is an unknown

and arbitrary correlation matrix.

Different from the model setting of [Figure 1](#), where Z_1, \dots, Z_m , are independently distributed Gaussian variables, we consider arbitrarily correlated Z_j and study dependence effect on the proposed method. To this end, we calibrate the dependence effect through the following procedure:

(a) Define

$$\bar{\rho} = \|\Sigma\|_1/m^2, \quad \text{where } \|\Sigma\|_1 = \sum_{ij} |\sigma_{ij}|;$$

and (b) introduce parameter η such that

$$\bar{\rho} = \bar{\rho}_m = m^{-\eta}, \quad \eta \in [0, 1]. \quad (9)$$

It can be seen that $\bar{\rho}$ summarizes the overall covariance dependence by calculating the mean absolute correlation. In high-dimensional data analysis with large m , $\bar{\rho}$ is often very close to zero because not every variable is correlated to all the other variables. For example, $\bar{\rho}$ of the $\Sigma_{m \times m}$ from an autoregressive model has the order of m^{-1} . In order to calibrate the dependence effect in a proper scale, we introduce the parameter η . Clearly, η is in a constant scale and decreases with $\bar{\rho}$. $\eta = 0$ corresponds to the extremely dependent case where every variable is correlated to all the other variables, and, at the opposite end, $\eta = 1$ corresponds to the independent case. In the literature, dependence conditions that are more general than (9) have been imposed for related inference problems such as multiple testing ([Fan et al., 2012](#)) and exact support recovery ([Gao and Stoev, 2020](#)). The new calibration in (9) enables the following joint analysis of signal sparsity and covariance effects for FNP control.

With γ and η representing signal sparsity and overall strength of covariance dependence, respectively, we discover a lower bound condition on the signal intensity (A_j) for the success of the proposed method. The lower bound is defined as

$$\mu_{min} = \min\{\mu_1, \mu_2\}, \quad (10)$$

where

$$\mu_1 = \sqrt{2\gamma \log m} \quad \text{and} \quad \mu_2 = \sqrt{(4\gamma - 2\eta)_+ \log m + 4 \log_3 m}.$$

Note that the lower bound μ_{min} increases with m at the order of $\sqrt{\log m}$. Such order is frequently required for signal intensity level in high-dimensional sparse inference (see, e.g., [Ingster \(1994\)](#), [Donoho and Jin \(2004\)](#), [Cai et al. \(2011\)](#), [Arias-Castro et al. \(2011\)](#), and [Cai and Sun \(2017a\)](#)). The term $\log_3 m (= \log \log \log m)$ is a technical term of an negligible order.

The lower bound μ_{min} takes the value of either μ_1 or μ_2 , depending on whichever is smaller under dependence. Specifically, $\mu_2 < \mu_1$ when η is large enough or, in other words, when covariance dependence is weak enough. As dependence gets stronger and η gets smaller, $\mu_1 < \mu_2$ and the lower bound equals to μ_1 and stops to change with η .

On the other hand, the lower bound μ_{min} depends on the signal sparsity parameter γ . The term $(4\gamma - 2\eta)_+$ can be zero for large enough γ , which means that the required signal intensity is only $\sqrt{4 \log_3 m}$ when signals are dense enough. For example, in the special case with independent variables, we have $\eta = 1$ and $(4\gamma - 2\eta)_+ = 0$ for $\gamma \leq 1/2$.

The following theorem shows the asymptotic performance of FNC screening when the lower bound condition is satisfied.

Theorem 2.1. *Consider model (8) and a user-specified control level β of FNP. Let $A_{min} = \min\{A_j, j \in I_1\}$ and assume $A_{min} - \mu_{min} \rightarrow \infty$ as $m \rightarrow \infty$, where μ_{min} is defined in (10). Then the FNC screening procedure with threshold $\hat{t}(\beta)$ defined in (6) efficiently controls the true FNP at the level of β , i.e.,*

$$P(FNP(\hat{t}(\beta)) \leq \beta) \rightarrow 1, \tag{11}$$

and, for any $\tilde{t} > \hat{t}(\beta)$,

$$P\{FNP(\tilde{t}) > \beta - \delta\} \rightarrow 1 \tag{12}$$

for arbitrarily small constant $\delta > 0$.

[Theorem 2.1](#) shows efficiency of FNC screening in selecting the smallest subset of variables

to achieve FNP control at the β level. In other words, the method also regulates unnecessary false positives to achieve the user-specified FNP control. The lower bound condition on A_{min} explicates the joint effect of signal intensity, signal sparsity, and covariance dependence on the FNC screening method.

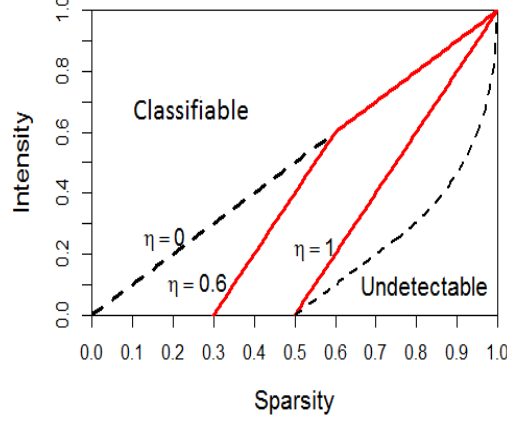


Figure 2: Signal retainable region of FNC screening under covariance dependence. Signals in the area above a solid red line can be retained by FNC screening at a pre-specified FNP level. The area increases with η as the dependence get weaker.

Utilizing the calibration of covariance dependence through η , we present the results of [Theorem 2.1](#) in a new phase diagram as follows. Let $A_{min} = \sqrt{2r \log m}$, $r > 0$. The condition on A_{min} in [Theorem 2.1](#) can be transformed to $r > \min\{\gamma, 2\gamma - \eta\}$ and demonstrated in a two-dimensional phase diagram with γ as the x axis and r as the y axis. The lower bound $\min\{\gamma, 2\gamma - \eta\}$ is illustrated in [Figure 2](#) by the red solid line that moves with the dependence parameter η . Signals in the area above the red solid line can be efficiently retained by FNC screening at a pre-specified level. Recall [Figure 1](#), which shows that under independence, signals in the region between the two dashed lines are only detectable for their existence but not classifiable. Our result in the special case of independence ($\eta = 1$) shows that many of such weak signals can be efficiently retained by the proposed method.

2.3 FNP control with estimated number of signals

Implementation of the proposed method requires information of the number of signals (s) which, in real applications, is often unknown. Existing studies for the estimation of s usually assume independence among variables (Genovese and Wasserman, 2004; Meinshausen and Rice, 2006; Cai et al., 2007; Cai and Jin, 2010), and most of them are for relatively dense signals. We are interested in finding an estimator of s that works in our setting with arbitrary covariance dependence. Recent study in Jeng (2021) introduces an estimator for the signal proportion $\pi(= s/m)$ with the form $\hat{\pi} = \max\{\hat{\pi}_\delta, \delta \in \Delta\}$, where Δ is a set of functions that render the most powerful consistent estimators in a family of estimators under different dependence scenarios. More specifically, the family of estimators are defined as

$$\hat{\pi}_\delta = \sup_{t>0} \frac{R(t)/m - 2\bar{\Phi}(t) - c_{m,\delta}\delta(t)}{1 - 2\bar{\Phi}(t)}, \quad (13)$$

where $\delta(t)$ is a strictly positive function on $(0, \infty)$ and $c_{m,\delta}$ is the bounding sequence corresponding to $\delta(t)$. It has been discovered that $\delta(t) = [\bar{\Phi}(t)]^{1/2}$ and $\delta(t) = \bar{\Phi}(t)$ result in powerful $\hat{\pi}_\delta$ under different dependence scenarios, and a new estimator is developed as

$$\hat{\pi} = \max\{\hat{\pi}_{0.5}, \hat{\pi}_1\}, \quad (14)$$

where $\hat{\pi}_{0.5}$ denotes $\hat{\pi}_\delta$ with $\delta = [\bar{\Phi}(t)]^{1/2}$, and $\hat{\pi}_1$ denotes $\hat{\pi}_\delta$ with $\delta = \bar{\Phi}(t)$. Details about the selection of $\delta(t)$, the construction of $c_{m,\delta}$, and the properties of $\hat{\pi}_\delta$ and $\hat{\pi}$ can be found in Jeng (2021).

We extend the results in Jeng (2021) to our setting with γ and η representing signal sparsity and overall dependence strength, respectively, so that the conditions for the consistency of $\hat{\pi}$ and the conditions for the FNP control of our proposed method can be unified. Because the theoretical analysis in Jeng (2021) is conducted on a discretized version ($\hat{\pi}_\delta^*$) of $\hat{\pi}_\delta$, which is defined by replacing $\sup_{t>0}$ in (13) with $\max_{t \in \mathbb{T}}$, where $\mathbb{T} = [1, \sqrt{5 \log m}] \cap \mathbb{N}$, we present the unified conditions for the discretized version of $\hat{\pi}$ as well and define it as $\hat{\pi}^* = \max\{\hat{\pi}_{0.5}^*, \hat{\pi}_1^*\}$.

Proposition 2.1. Assume the same conditions as in [Theorem 2.1](#). Then, for any constant $\epsilon > 0$,

$$P((1 - \epsilon) < \hat{\pi}^*/\pi < 1) \rightarrow 1. \quad (15)$$

Replace s in [\(6\)](#) with the estimator $\hat{s} = m \cdot \hat{\pi}^*$ and denote the selection threshold as $\hat{t}_s(\beta)$. We have

$$P(\text{FNP}(\hat{t}_s(\beta)) \leq \beta) \rightarrow 1 \quad (16)$$

and, for any threshold $\tilde{t} > \hat{t}_s(\beta)$,

$$P\{\text{FNP}(\tilde{t}) > \beta - \delta\} \rightarrow 1 \quad (17)$$

for arbitrarily small constant $\delta > 0$.

Proposition [Proposition 2.1](#) shows that the same set of conditions are sufficient for both the consistency of $\hat{\pi}^*$ and the efficient FNP control of FNC screening implemented with $\hat{\pi}^*$. This result can also be interpreted by the phase diagram in [Figure 2](#), where the solid red line that moves with the dependence level η now indicates the required signal intensity for both s estimation and FNP control. In other words, for signals above the solid red line, although they may not be indivily identifiable, we can still perform meaningful inference by not only estimating their total numbers but also effectively retaining them at a target FNP level.

Generally speaking, if we want to study the power of some method, a condition on the signal intensity is unavoidable. When signal intensity is too low, no methods can even detect their existence as illustrated in [Figure 1](#), let along the more challenging tasks of FNP control. When the condition on signal intensity does not hold, the estimator $\hat{\pi}$ tends to underestimate because of its lower bound property ([Jeng, 2021](#)). Consequently, FNC screening implemented with $\hat{s} = m \cdot \hat{\pi}$ tends to have a threshold higher than the ideal threshold that achieves the target level of β , which results in conservative variable selection with less false positives but inflated FNP. This tendency is observed in simulation examples with low signal-to-noise ratio in [Section 3.2](#).

We note that FNC screening is closely related to the FNC-Reg approach in [Jeng and Chen](#)

(2019). However, these two methods are developed for different models (two-groups model vs. linear regression model) and are studied under very different conditions. Particularly, the success of FNC-reg requires specific conditions on variable dependence and signal sparsity to facilitate accurate precision matrix estimation and bias mitigation in linear regression. Moreover, FNC-reg uses a different estimator for the number of signals, whose consistency under arbitrary covariance dependence of the two-groups model is unclear.

2.4 Computational algorithms

We provide algorithms to calculate the bounding sequence $c_{m,\delta}$, to derive the proportion estimator $\hat{\pi}$ in (13), and to select variables by FNC screening.

Algorithm 1 Bounding sequence $c_{m,\delta}$

Input: N sets of p -values generated by the joint null distribution of $\{z_1, \dots, z_m\}$

Output: bounding sequences $c_{m,0.5}$ and $c_{m,1}$

1: **for** $a = 1, 2, \dots, N$ **do**

Rank the a -th set of p -values such that $p_{a,(1)} < p_{a,(2)} < \dots < p_{a,(m)}$

Compute

$$V_{a,0.5} = \max_{1 \leq j \leq m} \frac{|j/m - p_{a,(j)}|}{\sqrt{p_{a,(j)}}} \quad \text{and} \quad V_{a,1} = \max_{1 \leq j \leq m} \frac{|j/m - p_{a,(j)}|}{p_{a,(j)}}$$

2: **end for**

3: Compute $c_{m,0.5}$ as the $(1 - 1/\sqrt{\log m})$ -th quantile of the empirical distribution of $V_{a,0.5}, a = 1, \dots, N$ and compute $c_{m,1}$ as the $(1 - 1/\sqrt{\log m})$ -th quantile of the empirical distribution of $V_{a,1}, a = 1, \dots, N$.

The computation of $c_{m,\delta}$ in Algorithm 1 requires input of p -values generated by the joint null distribution. When the joint null distribution is unknown in real applications, we can often simulate the null p -values non-parametrically. For example, when $\{z_1, \dots, z_m\}$ are a set of test statistics for associations between a set of explanatory variables and a response variable, we may randomly shuffle only the sample of the response variable to remove potential associations with the explanatory variables and then calculate the test statistics. More details for such permutation approaches can be found in Westfall and Young (1993). We generate N sets of null p -values, where N is a predetermined large number, such

as 1000.

Algorithm 2 Signal Proportion Estimator

Input: p -values of the observed test statistics and bounding sequences $c_{m,0.5}$ and $c_{m,1}$

Output: a proportion estimate $\hat{\pi}$

- 1: Rank the variables by their p -values so that $p_{(1)} < p_{(2)} < \dots < p_{(m)}$
- 2: Compute

$$\hat{\pi}_{0.5} = \max_{1 \leq j \leq m} \frac{j/m - p_{(j)} - c_{m,0.5} \cdot \sqrt{p_{(j)}}}{1 - p_{(j)}} \quad \text{and} \quad \hat{\pi}_1 = \max_{1 \leq j \leq m} \frac{j/m - p_{(j)} - c_{m,1} \cdot p_{(j)}}{1 - p_{(j)}}$$

- 3: Obtain $\hat{\pi} = \max\{\hat{\pi}_{0.5}, \hat{\pi}_1\}$
-

Algorithm 3 Dual Control Procedure

Input: p -values of the observed test statistics, a user-specified β , and a proportion estimate $\hat{\pi}$

Output: a set of selected variables

- 1: Rank the variables by their p -values so that $p_{(1)} < p_{(2)} < \dots < p_{(m)}$
- 2: Compute $\hat{s} = \hat{\pi}m$
- 3: For $j = 1, 2, \dots, m$, compute

$$\widehat{FNP}_j = \max\{1 - j/\hat{s} + (m - \hat{s})p_{(j)}/\hat{s}, 0\}$$

- 4: Let $k = 1$
while $\widehat{FNP}_k \geq \beta$ **do** $k = k + 1$
end while
 - 5: Obtain variables ranked at $1, \dots, k - 1$
-

3 Simulation

We provide simulation examples to demonstrate the finite-sample performance of the proposed FNC screening procedure. In these examples, a series of variables are generated as

$$(Z_1, \dots, Z_m)^T \sim N((\mu_1, \dots, \mu_m)^T, \Sigma), \quad (18)$$

where $\mu_j = A \cdot 1\{j \in I_1\}$, and I_1 is a set of indices randomly sampled from $\{1, \dots, m\}$ with cardinality $s = |I_1| = m^{1-\gamma}$. We consider three commonly observed dependence structures:

- Model 1 [Autoregressive]: $\Sigma = (\sigma_{ij}^{(1)})$, where $\sigma_{ij}^{(1)} = \lambda^{|i-j|}$ for $1 \leq i, j \leq m$.
- Model 2 [Block dependence]: $\Sigma = \mathbf{I}_{m/k} \otimes \mathbf{D}$, where \mathbf{D} is a $k \times k$ matrix with diagonal entries 1 and off-diagonal entries r .
- Model 3 [Factor model]: $\Sigma = (\sigma_{ij}^{(3)})$, where $\sigma_{ij}^{(3)} = V_{ij}/\sqrt{V_{ii}V_{jj}}$ for $1 \leq i, j \leq m$, $\mathbf{V} = \tau \mathbf{h}\mathbf{h}^T + \mathbf{I}_m$ with $\tau \in (0, 1)$ and $\mathbf{h} \sim N(\mathbf{0}, \mathbf{I}_m)$.

For the parameters in Model 1-3, we set $\lambda = 0.2, k = 40, r = 0.5$, and $\tau = 0.5$. The corresponding values of η , calculated by (9) with $m = 2000$ or $10,000$, and $\gamma = 0.3$, are presented in Table 2. It shows that dependence is very weak in Model 1 [Autoregressive] with η close to 1, moderately weak in Model 2 [Block dependence] with η between 0.6 and 0.7, and very strong in Model 3 [Factor model] with η between 0.1 and 0.3.

Recall the lower bound condition on the signal intensity in (10): $\mu_{\min} = \min\{\mu_1, \mu_2\}$, where μ_1 depends on signal sparsity through γ , μ_2 depends on both signal sparsity and dependence through γ and η , respectively. We present the values of μ_1 , μ_2 , and μ_{\min} under different dependence models in Table 2.

Table 2: Values of the dependence parameter η and the values of μ_1 , μ_2 , and μ_{\min} in simulation examples with $\gamma = 0.3$.

		η	μ_1	μ_2	μ_{\min}
$m = 2,000$	Autoregressive	0.95	2.14	1.68	1.68
	Block dependence	0.60	2.14	1.68	1.68
	Factor model	0.22	2.14	2.94	2.14
$m = 10,000$	Autoregressive	0.96	2.35	1.79	1.79
	Block dependence	0.67	2.35	1.79	1.79
	Factor model	0.18	2.35	3.29	2.35

3.1 Comparison with multiple testing methods

We compare the proposed method with the classical BH-FDR procedure (Benjamini and Hochberg, 1995). Specifically, we show that the FNP control property of our method cannot be achieved by manipulating the nominal level of BH-FDR.

As shown in Table 2, when $m = 2,000$ and $\gamma = 0.3$, μ_{min} of the lower bound condition is in the range of $1.68 - 2.14$ for the three dependence models. In this section, we set the signal intensity $A = 2$ and 3 , apply FNC screening method with the s known to us, and present the realized FNP of FNC screening from 100 replications. The results are compared with those of BH-FDR in Table 3. We also compare the realized false discovery proportion (FDP) of the two methods. Both methods are applied with varying nominal levels.

Table 3: Mean values and standard deviations (in brackets) of the realized FNP and FDP of the proposed FNC screening (FNCS) method and the existing BH-FDR procedure. This set of examples have $m = 2000$ and $\gamma = 0.3$.

			FNP	FDP
A=2	Autoregressive	FNCS($\beta = 0.2$)	0.201 (0.069)	0.576 (0.073)
		FNCS($\beta = 0.1$)	0.114 (0.069)	0.688 (0.085)
		BH-FDR($\alpha = 0.05$)	0.889 (0.035)	0.040 (0.043)
		BH-FDR($\alpha = 0.2$)	0.630 (0.050)	0.181 (0.044)
	Block dependence	FNCS($\beta = 0.2$)	0.193 (0.132)	0.607 (0.161)
		FNCS($\beta = 0.1$)	0.132 (0.116)	0.685 (0.152)
		BH-FDR($\alpha = 0.05$)	0.894 (0.058)	0.055 (0.070)
		BH-FDR($\alpha = 0.2$)	0.647 (0.097)	0.182 (0.093)
	Factor model	FNCS($\beta = 0.2$)	0.188 (0.169)	0.642 (0.107)
		FNCS($\beta = 0.1$)	0.156 (0.159)	0.693 (0.098)
		BH-FDR($\alpha = 0.05$)	0.886 (0.088)	0.032 (0.061)
		BH-FDR($\alpha = 0.2$)	0.659 (0.088)	0.160 (0.123)
A=3	Autoregressive	FNCS($\beta = 0.2$)	0.198 (0.023)	0.149 (0.035)
		FNCS($\beta = 0.1$)	0.101 (0.037)	0.307 (0.084)
		BH-FDR($\alpha = 0.05$)	0.378 (0.040)	0.044 (0.018)
		BH-FDR($\alpha = 0.2$)	0.166 (0.028)	0.183 (0.028)
	Block dependence	FNCS($\beta = 0.2$)	0.170 (0.086)	0.259 (0.247)
		FNCS($\beta = 0.1$)	0.089 (0.074)	0.444 (0.268)
		BH-FDR($\alpha = 0.05$)	0.387 (0.071)	0.047 (0.036)
		BH-FDR($\alpha = 0.2$)	0.169 (0.049)	0.180 (0.070)
	Factor model	FNCS($\beta = 0.2$)	0.160 (0.099)	0.262 (0.215)
		FNCS($\beta = 0.1$)	0.084 (0.104)	0.533 (0.227)
		BH-FDR($\alpha = 0.05$)	0.400 (0.043)	0.041 (0.049)
		BH-FDR($\alpha = 0.2$)	0.176 (0.049)	0.170 (0.113)

It can be seen that the mean values of FNP for FNC screening are generally closer to their corresponding nominal levels ($\beta = 0.2$ and 0.1) with larger A values. As dependence gets stronger from Model 1 [Autoregression] to Model 2 [Block dependence], to Model 3

[Factor model], not only the differences between the realized FNP and the nominal levels increases, but the standard deviations of the realized FNP increases as well. In other words, effective control of FNP by FNC screening becomes harder under stronger dependence. These observations agree with the theoretical results in Section 2.2.

On the other hand, Table 3 shows that the mean values of the realized FDP of BH-FDR are fairly close to their corresponding nominal levels of α . However, the mean values of FNP for BH-FDR are generally larger than those of FNC screening. It is true that one can increase the nominal level of BH-FDR to reduce FNP, but it is unclear by how much one should increase α to achieve a target level of FNP. For example, suppose we have a target $\beta = 0.2$. It seems that when $A = 3$, BH-FDR with $\alpha = 0.2$ has the mean values of FNP in the range of $0.166 - 0.176$, which are close to the target β . However, when $A = 2$, BH-FDR with $\alpha = 0.2$ has mean values of FNP in the range of $0.63 - 0.66$, which are much bigger than $\beta = 0.2$. Analogous results for $m = 10,000$ and $\gamma = 0.3$ are presented in Appendix 7.5.

These results demonstrate the fundamental differences between the existing multiple testing procedures and the proposed FNC screening method as they serve for very different purposes. The proposed method aims to efficiently retain signals at a target FNP level, for which the multiple testing methods cannot achieve. On the other hand, the new method pays the price of having a higher FDP when signals are relatively weak.

3.2 Comparison with other false negative control methods

In this section, we compare the empirical performances of FNC screening with existing methods that are designed to regulate false negatives. Among the existing methods discussed in Section 2, AFNC and MDR are more comparable to FNC screening because they all consider the two-groups model as in (1) and require the input of a user-specified control level. Moreover, they all require an estimate for the number of signals. For a fair comparison, we implement the same estimator $\hat{s} = m \cdot \hat{\pi}$, where $\hat{\pi}$ is defined in (14), to these methods.

The performances of the methods are evaluated by three measures. The first two measures, FNP and FDP are the same as in Table 3. The last measure is the Fowlkes-Mallows index (Fowlkes and Mallows, 1983; Halkidi et al., 2001), which summarizes the measures of

FNP and FDP by calculating the geometric mean of $(1-\text{FNP})$ and $(1-\text{FDP})$, i.e.,

$$\text{FM-index} = \sqrt{(1 - \text{FNP}) \times (1 - \text{FDP})}.$$

Higher values of the FM-index indicate better classification results. The FM-index is a sensible summary measure in high-dimensional settings with sparse alternative cases because the scale of FDP is more comparable to that of FNP than the classical false positive proportion ($\text{FPP} = \text{number of false positives}/\text{number of null cases}$). Because the methods presented in this section all focus on false negative control, it is appropriate to use FM-index to compare their efficiency.

In this section, variables are generated by (18) with $m = 2,000$ and a covariance matrix that has 20 diagonal blocks with block sizes randomly generated from 10 to 100. The non-zero off-diagonal correlations are set at 0.5. The dependence parameter η varies from sample to sample due to the random block size.

In the first set of examples, signal sparsity is fixed with $\gamma = 0.3$, and signal intensity (A) increases from 3 to 5. First, because the estimator \hat{s} underestimates the true s when signal intensity is not strong enough, FNC screening implemented with \hat{s} selects less variables than actually needed to reach the nominal level of β . These result in inflated realized FNP as seen in Table 4. Further, as A increases, the mean value of FNP of FNC screening gets closer to the nominal level of β , which agrees with the claims in (16) and (17) in Proposition 2.1. Among the three methods presented in Table 4, FNC screening shows a clear tendency to adapt to the nominal level of β as A increases, which is not observed for the other two methods. In terms of the FM-index, FNC screening generally outperforms the other two methods especially when signal intensity gets stronger.

In the second set of examples, signal intensity is fixed at 5 and signal sparsity γ increases from 0.3 to 0.5, so that the number of signals decreases from 205 to 45. The nominal level of β also varies. Results summarized in Table 5 show that FNC screening continues to outperform the other two methods in adapting to different nominal levels and incurring less false positives. Its advantage seems to be more prominent when signals get more sparse.

Table 4: Effect of signal intensity on different FN control methods. Mean values and standard deviations (in brackets) of the realized FNP, FDP, and the FM-index are presented for the proposed FNC screening method and two existing methods, AFNC and MDR from 100 replications.

		FNP	FDP	FM-index
$A = 3$	FNCS($\beta = \mathbf{0.1}$)	0.28 (0.12)	0.13 (0.14)	0.78 (0.04)
	AFNC($\beta = \mathbf{0.1}$)	0.19 (0.11)	0.22 (0.18)	0.78 (0.07)
	MDR($\beta = \mathbf{0.1}$)	0.09 (0.08)	0.49 (0.26)	0.65 (0.15)
$A = 4$	FNCS($\beta = \mathbf{0.1}$)	0.16 (0.07)	0.06 (0.12)	0.88 (0.05)
	AFNC($\beta = \mathbf{0.1}$)	0.07 (0.04)	0.14 (0.18)	0.89 (0.10)
	MDR($\beta = \mathbf{0.1}$)	0.06 (0.05)	0.37 (0.32)	0.74 (0.18)
$A = 5$	FNCS($\beta = \mathbf{0.1}$)	0.10 (0.04)	0.04 (0.12)	0.93 (0.06)
	AFNC($\beta = \mathbf{0.1}$)	0.01 (0.01)	0.36 (0.35)	0.75 (0.26)
	MDR($\beta = \mathbf{0.1}$)	0.04 (0.04)	0.36 (0.33)	0.75 (0.19)

4 Application in GWAS

Since established in early 2000s, GWAS have been very successful in identifying genetic variants that predispose to complex traits and diseases, often by accumulating very large sample sizes (Hu et al., 2021; Mikhaylova et al., 2021; Zhao et al., 2022; Mahajan et al., 2022). Yet, GWAS of many diseases remain underpowered, especially for non-European ancestries (Sun et al., 2022; Liu et al., 2022). In this application example, we demonstrate the potential power gain of a two-stage GWAS procedure that is empowered by the proposed FNC screening method.

To mimic under-powered GWAS, we randomly selected a limited number of European ancestry individuals from UK Biobank as our study samples, where ancestries were determined as in (Sun et al., 2022). We in total included 29 blood cell traits (same traits as included in Vuckovic et al. (2020)) and 5 randomly selected genome regions (3-4MB each), resulting in $29 \times 5 (= 145)$ trait-region combinations/datasets with sample size $n = 5000$. For each dataset, we first applied standard GWAS with Bonferroni correction. The GWAS summary statistics were obtained using the *regenie* software (Mbatchou et al., 2021) with linear mixed models. Covariates including age, sex, the first 10 genetic PCs, genotype array and recruitment centers are adjusted as in (Sun et al., 2022). The Bonferroni correction was conducted at the level of α/m_k , where α is the family-wise error rate and m_k is the

Table 5: Effect of nominal level and signal sparsity on different FN control methods.

		FNP	FDP	FM-index
$\gamma = 0.3$	FNCS($\beta = \mathbf{0.1}$)	0.10 (0.04)	0.04 (0.12)	0.93 (0.06)
	AFNC($\beta = \mathbf{0.1}$)	0.01 (0.01)	0.36 (0.35)	0.75 (0.26)
	MDR($\beta = \mathbf{0.1}$)	0.04 (0.04)	0.36 (0.33)	0.75 (0.19)
	FNCS($\beta = \mathbf{0.2}$)	0.19 (0.06)	0.02 (0.08)	0.89 (0.03)
	AFNC($\beta = \mathbf{0.2}$)	0.01 (0.01)	0.21 (0.29)	0.86 (0.20)
	MDR($\beta = \mathbf{0.2}$)	0.08 (0.09)	0.26 (0.28)	0.80 (0.14)
$\gamma = 0.5$	FNCS($\beta = \mathbf{0.1}$)	0.09 (0.05)	0.15 (0.29)	0.85 (0.18)
	AFNC($\beta = \mathbf{0.1}$)	0.00 (0.01)	0.73 (0.28)	0.44 (0.27)
	MDR($\beta = \mathbf{0.1}$)	0.03 (0.05)	0.56 (0.44)	0.54 (0.34)
	FNCS($\beta = \mathbf{0.2}$)	0.16 (0.09)	0.12 (0.27)	0.83 (0.15)
	AFNC($\beta = \mathbf{0.2}$)	0.01 (0.02)	0.60 (0.36)	0.55 (0.31)
	MDR($\beta = \mathbf{0.2}$)	0.07 (0.10)	0.54 (0.45)	0.54 (0.32)

dependence-adjusted number of tests for the k th dataset. More specifically, we utilized the linkage disequilibrium (LD) information from TOP-LD (Huang et al., 2022) Europeans as reference to approximate the number of independent tests to determine m_k . For all the 145 datasets, no significant variants were identified by the standard GWAS approach with $\alpha = 0.05$ due to the limited sample size.

To increase power of the study, we applied a new two-stage procedure empowered by the proposed FNC screening. The two-stage procedure adopts a standard framework in which all the variants are investigated in stage 1 using part of the available samples, and a proportion of the variants are followed up in stage 2 using the remaining samples. The two-stage framework can be tailored to achieve the same α level for family-wise error control as achieved by the standard one-stage GWAS (Skol et al., 2006). We propose to implement FNC screening in stage 1 using a minor part of the samples and only follow up with the selected variants in stage 2 with Bonferroni correction. The workflow is illustrated in Figure 3. While adopting the same $\alpha = 0.05$, the new procedure identified 149 significant variants from 35 datasets, in contrast to no significant variants by the standard one-stage GWAS.

To further justify these findings, we obtained the GWAS summary statistics based on 500,000 UKB European samples from Vuckovic et al. (2020), one of the largest GWAS for blood cell traits, which performed the standard one-stage GWAS including the same

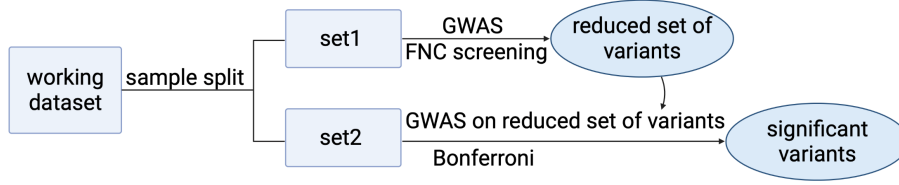


Figure 3: Workflow of the new two-stage procedure for one trait-region dataset. We randomly partitioned the $n = 5000$ working samples into two sets: a smaller set1 with size $n_1 = 1,500$ and a larger set2 with size $n_2 = 3,500$. In stage 1, we use set1 to derive GWAS summary statistics and apply FNC screening with $\beta = 0.1$. In stage 2, we use set2 to derive GWAS summary statistics and apply Bonferroni correction only on the variants selected in stage 1.

145 trait-region combinations with samples size $N = 500k$. We found that out of the 149 candidate variants selected by our two-stage method using the $n = 5000$ working samples, 114 are also present in Vuckovic et al. (2020), and 9 were identified as significant by the one-stage GWAS using the large validation data (panel a of Figure 4). Besides the 9 variants, the other candidate variants mostly have very small validation p-values as shown in panel b of Figure 4.

Panel c and d illustrate two examples comparing GWAS p-values of all the variants for the 5000 working samples with the GWAS p-values for the 500k validation samples. Data points of the candidate variants selected by our two-stage method for the 5000 working samples are highlighted by large cyan triangles. It can be seen that although the general pattern of the p-values does not show good consistency across the two datasets (due to limited sample size of the working data), most of the highlighted variants are supported by the validation p-values and are likely to be true signals.

The proposed two-stage procedure essentially benefits from pooling information of all signals to effectively reduce data dimension in the FNC screening step. Its power gain is more prominent when there are a relatively large number of weak signals. Such tendency is observed in the analysis of the 145 working datasets. For instance, the results presented in panel c and d of Figure 4 have $\hat{\pi} = 0.021$ and 0.028, respectively, corresponding to 279 and 372 signals. On the other hand, for datasets with very small signal proportion estimates, power gain of the two-stage procedure is not validated as well. Caution should be used for results with extremely small $\hat{\pi}$. Moreover, the two-stage procedure in this example adopted

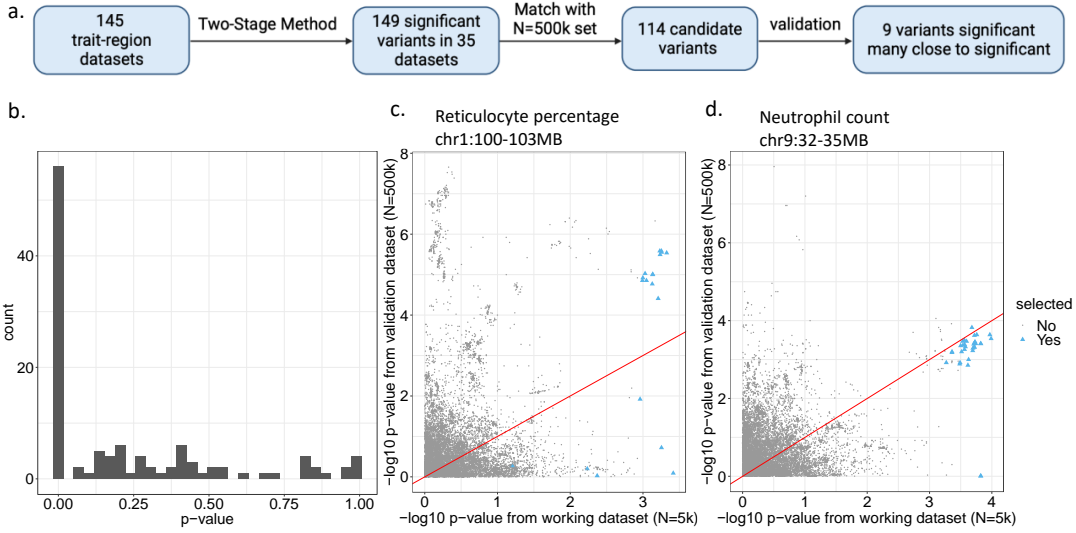


Figure 4: Two-stage GWAS analysis results. (a) Result summary. (b) Histogram of the validation p -values from the 500k samples for variants selected by the two-stage procedure. (c)(d) Comparison of $-\log_{10} p$ -values from a working dataset with 5,000 samples (x -axis) and $-\log_{10} p$ -values from the corresponding validation dataset with 500k samples (y -axis); (c) is for HLS reticulocyte percentage and chr1:100-103 MB and (d) is for neutrophil count and chr9:32-35 MB. Each point represents a genetic variant. Candidate variants selected by our two-stage procedure are highlighted by large triangles.

a 3:7 sample split as used in [Skol et al. \(2006\)](#) and a default β level. It will be interesting to develop data-driven strategies to determine the sample split ratio and the β level to optimize the power of the two-stage procedure.

5 Conclusion and Discussion

Motivated by the inquiries of weak signal in underpowered GWASs, we develop a new analytic framework to perform inference on signals that are detectable yet unidentifiable and propose the FNC screening method to efficiently control FNP at a user-specified level.

FNC screening is developed under arbitrary covariance dependence calibrated through a dependence parameter whose scale is compatible with the existing phase diagram in high-dimensional sparse inference. Utilizing the new calibration, we are able to explicate the joint effects of covariance dependence, signal sparsity, and signal intensity and interpret the results through a new phase diagram to gain important insight. The implementation of FNC

screening does not require any information of the dependence between variables, and the method is shown to be most powerful under independence. We note that if some dependence related data features are known a priori, more powerful method may be developed by leveraging the dependence information, which could result in larger signal retainable regions under dependence.

We demonstrate the finite sample performance of FNC screening in simulation under different dependence structures. It shows that FNC screening is able to effectively retain signals at a target FNP level, for which multiple testing methods cannot achieve. On the other hand, FNC screening outperforms other false negative control methods in adapting to different nominal levels and incurring less false positives under dependence.

In a real application example, we apply FNC screening to empower a standard two-stage procedure for GWAS. The empowered procedure demonstrates substantial power gain when working with limited sample size, which could help to alleviate critical issues in underpowered studies for minority populations. Future research on data-driven strategies to determine the sample split ratio and the β level in the first stage is of great interest. In general, the proposed FNC screening will be useful in applications where false negative results substantially hinder scientific investigations. Although such examples are abundant in real life, method development has been quite limited. Our study provides an insightful approach to bridge the important methodological gap.

6 Acknowledgment

This study has been conducted using the UK Biobank Resource under Application Number 25953. Research of Dr. Li is partially supported by NIH grant R01HL146500.

7 Appendix

This section provides the proofs of [Theorem 2.1](#) and [Proposition 2.1](#), and simulation results with $m = 10,000$.

We will frequently use the following result on Mill's ratio:

$$\bar{\Phi}(x) \leq x^{-1}\phi(x) \quad \text{for any } x > 0.$$

The symbol C denotes a genetic, finite constant whose value can be different at different occurrences.

7.1 Proof of Theorem 2.1

First, we show that $\widehat{\text{FNP}}(t)$ can accurately approximate $\text{FNP}(t)$ when t is large enough. Proof of the following lemma is provided in Appendix 7.2.

Lemma 7.1. *Consider model (8). For any $t = t_m \geq \mu_{\min}$, where μ_{\min} is defined in (10), we have*

$$|\widehat{\text{FNP}}(t) - \text{FNP}(t)| = o_P(1). \quad (19)$$

Then, by Markov's inequality, for a fixed constant $a > 0$,

$$\begin{aligned} P(\text{FNP}(\mu_{\min}) > a) &= P(s^{-1} \sum_{j \in I_1} 1_{\{Z_j \leq \mu_{\min}\}} > a) \\ &\leq \frac{1}{as} \sum_{j \in I_1} P(Z_j \leq \mu_{\min}) \\ &\leq \frac{1}{a} \max_{j \in I_1} P(N(0, 1) \leq \mu_{\min} - A_j) \\ &\leq \frac{1}{a} \max_{j \in I_1} P(N(0, 1) \leq \mu_{\min} - A_{\min}) = o(1), \end{aligned}$$

where the last step is by the condition on A_{\min} . Therefore, $\text{FNP}(\mu_{\min}) = o_P(1)$. By Lemma 7.1, we have $|\widehat{\text{FNP}}(\mu_{\min}) - \text{FNP}(\mu_{\min})| = o_P(1)$, which implies $\widehat{\text{FNP}}(\mu_{\min}) = o_P(1)$ and $\widehat{\text{FNP}}(\mu_{\min}) < \beta$ with probability tending to 1. Recall the construction of $\hat{t}(\beta)$: $\hat{t}(\beta) = \sup \{t : \widehat{\text{FNP}}(t) < \beta\}$, we have $P(\hat{t}(\beta) \geq \mu_{\min}) \rightarrow 1$. Consequently, since $\hat{t}(\beta)$ is random,

$$\begin{aligned}
& \lim_{m \rightarrow \infty} P(|\widehat{\text{FNP}}(\hat{t}(\beta)) - \text{FNP}(\hat{t}(\beta))| > a) \\
&= \lim_{m \rightarrow \infty} E \left[E \left(1_{\{|\widehat{\text{FNP}}(\hat{t}(\beta)) - \text{FNP}(\hat{t}(\beta))| > a\}} | \hat{t}(\beta) \right) \right] \\
&= E \left[\lim_{m \rightarrow \infty} E \left(1_{\{|\widehat{\text{FNP}}(\hat{t}(\beta)) - \text{FNP}(\hat{t}(\beta))| > a\}} | \hat{t}(\beta) \right) \right] \\
&= 0,
\end{aligned}$$

where the second step above is by dominated convergence theorem and the last step is by Lemma 7.1. Therefore, $|\widehat{\text{FNP}}(\hat{t}(\beta)) - \text{FNP}(\hat{t}(\beta))| = o_P(1)$. Now, since $\widehat{\text{FNP}}(\hat{t}(\beta)) < \beta$ almost surely by the construction of $\hat{t}(\beta)$, claim in (11) follows.

Next, let's consider the claim in (12). Because $\tilde{t} > \hat{t}(\beta)$, the construction of $\hat{t}(\beta)$ implies that $\widehat{\text{FNP}}(\tilde{t}) \geq \beta$ almost surely. On the other hand, because $t > \hat{t}(\beta) \geq \mu_{\min}$ with probability tending to 1, similar arguments as the above lead to $|\widehat{\text{FNP}}(\tilde{t}) - \text{FNP}(\tilde{t})| = o_P(1)$. Therefore, the claim in (12) follows.

7.2 Proof of Lemma 7.1

For notation simplicity, let

$$B(t) = 1 - R(t)/s + (m - s)\bar{\Phi}(t)/s. \quad (20)$$

Then $\widehat{\text{FNP}}(t) = \max\{B(t), 0\}$, and it is sufficient to show that

$$|B(t) - \text{FNP}(t)| = o_P(1) \quad \text{when } B(t) \geq 0 \quad (21)$$

and

$$\text{FNP}(t) = o_P(1) \quad \text{when } B(t) < 0. \quad (22)$$

Consider (21) first. By the definitions of $B(t)$ and $\text{FNP}(t)$,

$$\begin{aligned} |B(t) - \text{FNP}(t)| &= |s^{-1}(\mathbf{R}(t) - (m - s)\bar{\Phi}(t)) - s^{-1}(\mathbf{R}(t) - \text{FP}(t))| \\ &= s^{-1}|\text{FP}(t) - (m - s)\bar{\Phi}(t)|. \end{aligned}$$

Therefore, it is sufficient to show

$$s^{-1}|\text{FP}(t) - (m - s)\bar{\Phi}(t)| = o_P(1). \quad (23)$$

Recall the definition of μ_1 and μ_2 in (10). The following proof is composed of two parts. The first part assumes $t \geq \mu_1$ and the second part assumes $\mu_2 \leq t < \mu_1$.

Consider the first part. It's sufficient to show $s^{-1}\text{FP}(t) = o_P(1)$ and $s^{-1}(m - s)\bar{\Phi}(t) = o(1)$ with $t \geq \mu_1$. By Mill's ratio and the re-parameterization of s in γ ,

$$s^{-1}(m - s)\bar{\Phi}(t) \leq \frac{Cme^{-t^2/2}}{ts} \leq \frac{C}{\sqrt{\log m}} = o(1).$$

On the other hand, for a fixed constant $a > 0$,

$$P(s^{-1}\text{FP}(t) > a) \leq \frac{E(\text{FP}(t))}{as} \leq \frac{m\bar{\Phi}(t)}{as} = o(1).$$

Therefore, the claim in (23) is justified for $t \geq \mu_1 = \sqrt{2\gamma \log m}$.

Next we present the second part of the proof with $\mu_2 \leq t < \mu_1$. Define

$$D_m = s^{-2}e^{-t^2/2}\|\Sigma\|_1 \log_2 m.$$

Apply the re-parameterizations of $\|\Sigma\|_1$ in η and s in γ , we have

$$D_m = m^{2\gamma-\eta}e^{-t^2/2} \log_2 m.$$

By the condition $t \geq \mu_2$, direct calculation gives

$$m^{2\gamma-\eta}e^{-t^2/2}\log_2 m \leq \log_2^{-1} m = o(1).$$

Then, $D_m = o(1)$ and (23) is implied by

$$s^{-1}|\text{FP}(t) - (m-s)\bar{\Phi}(t)| = o_P(\sqrt{D_m}). \quad (24)$$

Apply Chebyshev's inequality,

$$P(s^{-1}|\text{FP}(t) - (m-s)\bar{\Phi}(t)| > \sqrt{D_m}) \leq \frac{\text{Var}(\text{FP}(t))}{s^2 D_m}. \quad (25)$$

We have the following lemma for the order of $\text{Var}(\text{FP}(t))$ under dependence. The proof is provided in Section 7.3.

Lemma 7.2. *Consider model (8). Denote Σ_0 as the correlation matrix of $Z_j, j \in I_0$. We have*

$$\text{Var}\left(\sum_{j \in I_0} 1_{\{Z_j > t\}}\right) = O(e^{-t^2/2} \|\Sigma_0\|_1). \quad (26)$$

Therefore, $\text{Var}(\text{FP}(t)) = \text{Var}(\sum_{j \in I_0} 1_{\{Z_j > t\}}) \leq Ce^{-t^2/2} \|\Sigma_0\|_1 \leq Ce^{-t^2/2} \|\Sigma\|_1$, and it follows that

$$\frac{\text{Var}(\text{FP}(t))}{s^2 D_m} = o(1) \quad (27)$$

by the definition of D_m . Combining (25) and (27) gives (24), which justifies the claim in (23) for $\mu_2 \leq t < \mu_1$.

Finally, consider (22). It can be shown that $B(t) < 0$ implies $1 - \text{FP}(t)/s - \text{TP}(t)/s + (m-s)\bar{\Phi}(t)/s < 0$, which, combined with $\text{FNP}(t) = 1 - \text{TP}(t)/s$, further implies

$$\text{FNP}(t) < s^{-1}(\text{FP}(t) - (m-s)\bar{\Phi}(t)).$$

Since the order of the right hand side has been derived in (23), (22) follows.

7.3 Proof of Lemma 7.2

$$\text{Var}\left(\sum_{j \in I_0} 1_{\{Z_j > t\}}\right) = \sum_{j=1}^m \text{Var}(1_{\{Z_j > t\}}) + \sum_{i \neq j} \text{Cov}(1_{\{Z_i > t\}}, 1_{\{Z_j > t\}}).$$

By Mill's ratio,

$$\sum_{j=1}^m \text{Var}(1_{\{Z_j > t\}}) \leq m\bar{\Phi}(t)(1 - \bar{\Phi}(t)) \leq Cme^{-t^2/2}.$$

For $\sum_{i \neq j} \text{Cov}(1_{\{Z_i > t\}}, 1_{\{Z_j > t\}})$, we have

$$\text{Cov}(1_{\{Z_i > t\}}, 1_{\{Z_j > t\}}) = \int_{-\infty}^t \int_{-\infty}^t f(x, y) dx dy - \int_{-\infty}^t \phi(x) dx \int_{-\infty}^t \phi(y) dy \leq C|\Sigma_{ij}|e^{-t^2/2},$$

where the last step follows from Corollary 2.1 in Li and Shao (2002). Combining the above results in (26).

7.4 Proof of Proposition 2.1

The consistency of $\hat{\pi}^*$ is based on the following two lemmas, which are implied by Theorem 2.2 and 2.3 in Jeng (2021).

Lemma 7.3. *Consider model (8). Let $\delta(t) = [\bar{\Phi}(t)]^{1/2}$. Then, there exists a bounding sequence $c_{m,\delta}^* = O(\sqrt{\bar{\rho} \cdot \log m})$, and the corresponding estimator $\hat{\pi}_\delta^*$ satisfies $P(\hat{\pi}_\delta^* < \pi) \rightarrow 1$. Moreover, for π satisfying $0 < \pi \ll 1$, if $A_{\min} \gg 1$ and*

$$A_{\min} - \bar{\Phi}^{-1}\left(\frac{\pi^2}{\bar{\rho} \cdot \log m}\right) \rightarrow \infty, \quad (28)$$

then $P(\hat{\pi}_\delta^ > (1 - \epsilon)\pi) \rightarrow 1$ for any constant $\epsilon > 0$.*

Lemma 7.4. *Consider model (8). Let $\delta(t) = \bar{\Phi}(t)$. Then, there exists a bounding sequence $c_{m,\delta}^* = O(\sqrt{\log m})$, and the corresponding estimator $\hat{\pi}_\delta^*$ satisfies $P(\hat{\pi}_\delta^* < \pi) \rightarrow 1$. Moreover,*

for π satisfying $0 < \pi \ll 1$, if $A_{min} \gg 1$ and

$$A_{min} - \bar{\Phi}^{-1} \left(\frac{\pi}{\sqrt{\log m}} \right) \rightarrow \infty. \quad (29)$$

then $P(\hat{\pi}_\delta^* > (1 - \epsilon)\pi) \rightarrow 1$ for any constant $\epsilon > 0$.

Recall that $\pi = m^{-\gamma}$, $\gamma \in (0, 1)$, and $\bar{\rho} = m^{-\eta}$, $\eta \in [0, 1]$. Recall μ_1 and μ_2 in (10). Direct calculation shows that when $A_{min} - \mu_2 \rightarrow \infty$, the condition in (28) is satisfied, and when $A_{min} - \mu_1 \rightarrow \infty$, the condition in (29) is satisfied. Therefore, given $A_{min} - \mu_{min} \rightarrow \infty$, the consistency of the estimator $\hat{\pi}^* = \max\{\hat{\pi}_{0.5}^*, \hat{\pi}_1^*\}$ holds as in (15).

Next consider the claims in (16) and (17). Similar arguments as in the proof of Theorem 2.1 can be applied, and we only need to show that Lemma 7.1 continues to hold with $\widehat{\text{FNP}}(t)$ replaced by $\widehat{\text{FNP}}_{\hat{s}}(t)$. Given the result in (19), it is sufficient to show $|\widehat{\text{FNP}}_{\hat{s}}(t) - \widehat{\text{FNP}}(t)| = o_P(1)$ for $t = t_m \geq \mu_{min}$, which, by the definition of $B(t)$ in (20), is implied by

$$|B_{\hat{s}}(t) - B(t)| = o_P(1) \quad \text{for } t = t_m \geq \mu_{min}. \quad (30)$$

By direct calculation,

$$\begin{aligned} |B_{\hat{s}}(t) - B(t)| &= |(\hat{s}^{-1} - s^{-1})(R(t) - m\bar{\Phi}(t))| \\ &\leq |\hat{s}^{-1} - s^{-1}| \cdot \text{TP}(t) + |\hat{s}^{-1} - s^{-1}| \cdot |\text{FP}(t) - m\bar{\Phi}(t)|. \end{aligned} \quad (31)$$

Given $P((1 - \delta) < \hat{s}/s < 1) \rightarrow 1$ for any $\delta > 0$, it can be shown that

$$\begin{aligned} P(|\hat{s}^{-1} - s^{-1}| < \frac{\delta}{1 - \delta} s^{-1}) &= P(|1 - \hat{s}/s| < \frac{\delta}{1 - \delta} \hat{s}/s) \\ &> P(0 < 1 - \hat{s}/s < \frac{\delta}{1 - \delta} \hat{s}/s) = P((1 - \delta) < \hat{s}/s < 1) \rightarrow 1. \end{aligned}$$

On the other hand, $\text{TP}(t) \leq s$ almost surely. Then it follows that the first term in (31),

$$|\hat{s}^{-1} - s^{-1}| \cdot \text{TP}(t) = o_P(1).$$

For the second term in (31),

$$\begin{aligned} |\hat{s}^{-1} - s^{-1}| \cdot |\text{FP}(t) - m\bar{\Phi}(t)| &< \frac{\delta}{1-\delta} s^{-1} |\text{FP}(t) - m\bar{\Phi}(t)| \\ &\leq \frac{\delta}{1-\delta} (s^{-1} |\text{FP}(t) - (m-s)\bar{\Phi}(t)| + \bar{\Phi}(t)) \end{aligned}$$

with probability tending to 1. Since $\bar{\Phi}(t) = o(1)$ for $t \geq \mu_{\min}$ and it has been shown as for (23) that $s^{-1} |\text{FP}(t) - (m-s)\bar{\Phi}(t)| = o_P(1)$ for $t \geq \mu_{\min}$, then it follows that

$$|\hat{s}^{-1} - s^{-1}| \cdot |\text{FP}(t) - m\bar{\Phi}(t)| = o_P(1).$$

Summing up the above gives (30).

7.5 Simulation results with $m = 10,000$

In this example, data are generated under the same setting as in Section 3.1 except that $m = 10,000$. Results presented in Table 6 show similar trends as in Table 3.

References

- Arias-Castro, E., E. J. Candès, and Y. Plan (2011). Global testing under sparse alternatives: Anova, multiple comparisons and the higher criticism. *The Annals of Statistics* 39(5), 2533–2556.
- Arias-Castro, E. and S. Chen (2017). Distribution-free multiple testing. *Electronic Journal of Statistics* 11(1), 1983–2001.
- Benjamini, Y. and Y. Hochberg (1995). Controlling the false discovery rate: a practical and powerful approach to multiple testing. *J. R. Statist. Soc. Ser. B* 57(1), 289–300.
- Cai, T., J. Jin, and M. Low (2007). Estimation and confidence sets for sparse normal mixtures. *The Annals of Statistics* 35(6), 2421–2449.

Table 6: Mean values and standard deviations (in brackets) of the realized FNP and FDP of the proposed FNC screening method and the existing BH-FDR procedure. This set of examples have $m = 10,000$ and $\gamma = 0.3$.

			FNP	FDP
A=2	Autoregressive	DCOE($\beta = \mathbf{0.2}$)	0.202 (0.048)	0.690 (0.048)
		DCOE($\beta = \mathbf{0.1}$)	0.111 (0.053)	0.784 (0.057)
		BH-FDR($\alpha = \mathbf{0.05}$)	0.935 (0.021)	0.045 (0.032)
		BH-FDR($\alpha = \mathbf{0.2}$)	0.736 (0.031)	0.189 (0.031)
	Block dependence	DCOE($\beta = \mathbf{0.2}$)	0.190 (0.121)	0.716 (0.120)
		DCOE($\beta = \mathbf{0.1}$)	0.126 (0.102)	0.783 (0.106)
		BH-FDR($\alpha = \mathbf{0.05}$)	0.935 (0.024)	0.049 (0.050)
		BH-FDR($\alpha = \mathbf{0.2}$)	0.740 (0.047)	0.190 (0.064)
	Factor model	DCOE($\beta = \mathbf{0.2}$)	0.199 (0.194)	0.738 (0.124)
		DCOE($\beta = \mathbf{0.1}$)	0.173 (0.86)	0.771 (0.110)
		BH-FDR($\alpha = \mathbf{0.05}$)	0.930 (0.061)	0.035 (0.051)
		BH-FDR($\alpha = \mathbf{0.2}$)	0.747 (0.086)	0.170 (0.135)
A=3	Autoregressive	DCOE($\beta = \mathbf{0.2}$)	0.202 (0.017)	0.221 (0.027)
		DCOE($\beta = \mathbf{0.1}$)	0.107 (0.026)	0.404 (0.078)
		BH-FDR($\alpha = \mathbf{0.05}$)	0.464 (0.025)	0.047 (0.011)
		BH-FDR($\alpha = \mathbf{0.2}$)	0.225 (0.018)	0.188 (0.016)
	Block dependence	DCOE($\beta = \mathbf{0.2}$)	0.185 (0.064)	0.277 (0.165)
		DCOE($\beta = \mathbf{0.1}$)	0.091 (0.065)	0.519 (0.235)
		BH-FDR($\alpha = \mathbf{0.05}$)	0.464 (0.035)	0.051 (0.025)
		BH-FDR($\alpha = \mathbf{0.2}$)	0.227 (0.025)	0.187 (0.045)
	Factor model	DCOE($\beta = \mathbf{0.2}$)	0.122 (0.132)	0.547 (0.282)
		DCOE($\beta = \mathbf{0.1}$)	0.089 (0.115)	0.641 (0.236)
		BH-FDR($\alpha = \mathbf{0.05}$)	0.472 (0.030)	0.041 (0.042)
		BH-FDR($\alpha = \mathbf{0.2}$)	0.232 (0.034)	0.180 (0.125)

Cai, T. T., X. J. Jeng, and J. Jin (2011). Optimal detection of heterogeneous and heteroscedastic mixtures. *Journal of the Royal Statistical Society: Series B (Statistical Methodology)* 73(5), 629–662.

Cai, T. T. and J. Jin (2010). Optimal rates of convergence for estimating the null density and proportion of nonnull effects in large-scale multiple testing. *The Annals of Statistics*, 100–145.

Cai, T. T. and W. Sun (2017a). Large-scale global and simultaneous inference: Estimation and testing in very high dimensions. *Annual Review of Economics* 9, 411–439.

- Cai, T. T. and W. Sun (2017b). Optimal screening and discovery of sparse signals with applications to multistage high-throughput studies. *Journal of the Royal Statistical Society: Series B* 79(1), 197–223.
- Chen, S. X., J. Li, and P.-S. Zhong (2019). Two-sample and anova tests for high dimensional means. *The Annals of Statistics* 47(3), 1443–1474.
- Donoho, D. and J. Jin (2004). Higher criticism for detecting sparse heterogeneous mixtures. *The Annals of Statistics* 32(3), 962–994.
- Donoho, D. and J. Jin (2015). Special invited paper: Higher criticism for large-scale inference, especially for rare and weak effects. *Statistical Science*, 1–25.
- Fan, J., X. Han, and W. Gu (2012). Estimating false discovery proportion under arbitrary covariance dependence. *J. Amer. Statist. Assoc.* 107(499), 1019–1035.
- Fowlkes, E. B. and C. L. Mallows (1983). A method for comparing two hierarchical clusterings. *Journal of the American statistical association* 78(383), 553–569.
- Gao, Z. and S. Stoev (2020). Fundamental limits of exact support recovery in high dimensions. *Bernoulli* 26(4), 2605–2638.
- Gao, Z. and S. Stoev (2021). *Concentration of Maxima and Fundamental Limits in High-Dimensional Testing and Inference*. Springer.
- Genovese, C. and L. Wasserman (2002). Operating characteristics and extensions of the false discovery rate procedure. *Journal of the Royal Statistical Society: Series B (Statistical Methodology)* 64(3), 499–517.
- Genovese, C. and L. Wasserman (2004). A stochastic process approach to false discovery control. *Annals of Statistics* 32, 1035–1061.
- Halkidi, M., Y. Batistakis, and M. Vazirgiannis (2001). On clustering validation techniques. *Journal of intelligent information systems* 17(2-3), 107–145.

- Hu, Y., A. M. Stilp, C. P. McHugh, S. Rao, D. Jain, X. Zheng, J. Lane, S. Méric de Bellefon, L. M. Raffield, M.-H. Chen, L. R. Yanek, M. Wheeler, Y. Yao, C. Ren, J. Broome, J.-Y. Moon, P. S. de Vries, B. D. Hobbs, Q. Sun, P. Surendran, J. A. Brody, T. W. Blackwell, H. Choquet, K. Ryan, R. Duggirala, N. Heard-Costa, Z. Wang, N. Chami, M. H. Preuss, N. Min, L. Ekunwe, L. A. Lange, M. Cushman, N. Faraday, J. E. Curran, L. Almasy, K. Kundu, A. V. Smith, S. Gabriel, J. I. Rotter, M. Fornage, D. M. Lloyd-Jones, R. S. Vasan, N. L. Smith, K. E. North, E. Boerwinkle, L. C. Becker, J. P. Lewis, G. R. Abecasis, L. Hou, J. R. O’Connell, A. C. Morrison, T. H. Beaty, R. Kaplan, A. Correa, J. Blangero, E. Jorgenson, B. M. Psaty, C. Kooperberg, R. T. Walton, B. P. Kleinstiver, H. Tang, R. J. F. Loos, N. Soranzo, A. S. Butterworth, D. Nickerson, S. S. Rich, B. D. Mitchell, A. D. Johnson, P. L. Auer, Y. Li, R. A. Mathias, G. Lettre, N. Pankratz, C. C. Laurie, C. A. Laurie, D. E. Bauer, M. P. Conomos, A. P. Reiner, and NHLBI Trans-Omics for Precision Medicine (TOPMed) Consortium (2021). Whole-genome sequencing association analysis of quantitative red blood cell phenotypes: The NHLBI TOPMed program. *Am. J. Hum. Genet.* 108(5), 874–893.
- Huang, L., J. D. Rosen, Q. Sun, J. Chen, M. M. Wheeler, Y. Zhou, Y.-I. Min, C. Kooperberg, M. P. Conomos, A. M. Stilp, S. S. Rich, J. I. Rotter, A. Manichaikul, R. J. F. Loos, E. E. Kenny, T. W. Blackwell, A. V. Smith, G. Jun, F. J. Sedlazeck, G. Metcalf, E. Boerwinkle, NHLBI Trans-Omics for Precision Medicine (TOPMed) Consortium, L. M. Raffield, A. P. Reiner, P. L. Auer, and Y. Li (2022). TOP-LD: A tool to explore linkage disequilibrium with TOPMed whole-genome sequence data. *Am. J. Hum. Genet.* 109(6), 1175–1181.
- Ingster, Y. I. (1994). Minimax detection of a signal in p metrics. *Journal of Mathematical Sciences* 68(4), 503–515.
- Jeng, X. J. (2021). Estimating the proportion of signal variables under arbitrary covariance dependence. *arXiv preprint arXiv:2102.09053*.
- Jeng, X. J. and X. Chen (2019). Variable selection via adaptive false negative control in linear regression. *Electron. J. Statist.* 13(2), 5306–5333.

- Jeng, X. J., Z. J. Daye, W. Lu, and J.-Y. Tzeng (2016). Rare variants association analysis in large-scale sequencing studies at the single locus level. *PLoS computational biology* 12(6).
- Jeng, X. J., T. Zhang, and J.-Y. Tzeng (2019). Efficient signal inclusion with genomic applications. *Journal of the American Statistical Association* 114, 1787–1799.
- Ji, P. and J. Jin (2012). Ups delivers optimal phase diagram in high-dimensional variable selection. *The Annals of Statistics* 40(1), 73–103.
- Ji, P. and Z. Zhao (2014). Rate optimal multiple testing procedure in high-dimensional regression. *arXiv preprint arXiv:1404.2961*.
- Jin, J., Z. T. Ke, and W. Wang (2017). Phase transitions for high dimensional clustering and related problems. *The Annals of Statistics* 45(5), 2151–2189.
- Li, W. V. and Q.-M. Shao (2002). A normal comparison inequality and its applications. *Probability Theory and Related Fields* 122(4), 494–508.
- Liu, W., Q. Sun, L. Huang, A. Bhattacharya, G. W. Wang, X. Tan, K. C. K. Kuban, R. M. Joseph, T. M. O’Shea, R. C. Fry, Y. Li, and H. P. Santos, Jr (2022). Innovative computational approaches shed light on genetic mechanisms underlying cognitive impairment among children born extremely preterm. *J. Neurodev. Disord.* 14(1), 16.
- Mahajan, A., C. N. Spracklen, W. Zhang, M. C. Y. Ng, L. E. Petty, H. Kitajima, G. Z. Yu, S. Rüeger, L. Speidel, Y. J. Kim, M. Horikoshi, J. M. Mercader, D. Taliun, S. Moon, S.-H. Kwak, N. R. Robertson, N. W. Rayner, M. Loh, B.-J. Kim, J. Chiou, I. Miguel-Escalada, P. Della Briotta Parolo, K. Lin, F. Bragg, M. H. Preuss, F. Takeuchi, J. Nano, X. Guo, A. Lamri, M. Nakatochi, R. A. Scott, J.-J. Lee, A. Huerta-Chagoya, M. Graff, J.-F. Chai, E. J. Parra, J. Yao, L. F. Bielak, Y. Tabara, Y. Hai, V. Steinthorsdottir, J. P. Cook, M. Kals, N. Grarup, E. M. Schmidt, I. Pan, T. Sofer, M. Wuttke, C. Sarnowski, C. Gieger, D. Noursome, S. Trompet, J. Long, M. Sun, L. Tong, W.-M. Chen, M. Ahmad, R. Noordam, V. J. Y. Lim, C. H. T. Tam, Y. Y. Joo, C.-H. Chen, L. M. Raffield, C. Lecoeur, B. P. Prins, A. Nicolas, L. R. Yanek, G. Chen, R. A. Jensen, S. Tajuddin, E. K.

Kabagambe, P. An, A. H. Xiang, H. S. Choi, B. E. Cade, J. Tan, J. Flanagan, F. Abaitua,
 L. S. Adair, A. Adeyemo, C. A. Aguilar-Salinas, M. Akiyama, S. S. Anand, A. Bertoni,
 Z. Bian, J. Bork-Jensen, I. Brandslund, J. A. Brody, C. M. Brummett, T. A. Buchanan,
 M. Canouil, J. C. N. Chan, L.-C. Chang, M.-L. Chee, J. Chen, S.-H. Chen, Y.-T. Chen,
 Z. Chen, L.-M. Chuang, M. Cushman, S. K. Das, H. J. de Silva, G. Dedoussis, L. Dimitrov,
 A. P. Doumatey, S. Du, Q. Duan, K.-U. Eckardt, L. S. Emery, D. S. Evans, M. K. Evans,
 K. Fischer, J. S. Floyd, I. Ford, M. Fornage, O. H. Franco, T. M. Frayling, B. I. Freed-
 man, C. Fuchsberger, P. Genter, H. C. Gerstein, V. Giedraitis, C. González-Villalpando,
 M. E. González-Villalpando, M. O. Goodarzi, P. Gordon-Larsen, D. Gorkin, M. Gross,
 Y. Guo, S. Hackinger, S. Han, A. T. Hattersley, C. Herder, A.-G. Howard, W. Hsueh,
 M. Huang, W. Huang, Y.-J. Hung, M. Y. Hwang, C.-M. Hwu, S. Ichihara, M. A. Ikram,
 M. Ingelsson, M. T. Islam, M. Isono, H.-M. Jang, F. Jasmine, G. Jiang, J. B. Jonas,
 M. E. Jørgensen, T. Jørgensen, Y. Kamatani, F. R. Kandeel, A. Kasturiratne, T. Kat-
 saya, V. Kaur, T. Kawaguchi, J. M. Keaton, A. N. Kho, C.-C. Khor, M. G. Kibriya, D.-H.
 Kim, K. Kohara, J. Kriebel, F. Kronenberg, J. Kuusisto, K. Läll, L. A. Lange, M.-S. Lee,
 N. R. Lee, A. Leong, L. Li, Y. Li, R. Li-Gao, S. Ligthart, C. M. Lindgren, A. Linneberg,
 C.-T. Liu, J. Liu, A. E. Locke, T. Louie, J. Luan, A. O. Luk, X. Luo, J. Lv, V. Lyssenko,
 V. Mamakou, K. R. Mani, T. Meitinger, A. Metspalu, A. D. Morris, G. N. Nadkarni,
 J. L. Nadler, M. A. Nalls, U. Nayak, S. S. Nongmaithem, I. Ntalla, Y. Okada, L. Orozco,
 S. R. Patel, M. A. Pereira, A. Peters, F. J. Pirie, B. Porneala, G. Prasad, S. Preissl,
 L. J. Rasmussen-Torvik, A. P. Reiner, M. Roden, R. Rohde, K. Roll, C. Sabanayagam,
 M. Sander, K. Sandow, N. Sattar, S. Schönherr, C. Schurmann, M. Shahriar, J. Shi, D. M.
 Shin, D. Shriner, J. A. Smith, W. Y. So, A. Stančáková, A. M. Stilp, K. Strauch, K. Suzuki,
 A. Takahashi, K. D. Taylor, B. Thorand, G. Thorleifsson, U. Thorsteinsdottir, B. Tomlin-
 son, J. M. Torres, F.-J. Tsai, J. Tuomilehto, T. Tusie-Luna, M. S. Udler, A. Valladares-
 Salgado, R. M. van Dam, J. B. van Klinken, R. Varma, M. Vujkovic, N. Wachter-Rodarte,
 E. Wheeler, E. A. Whitsel, A. R. Wickremasinghe, K. W. van Dijk, D. R. Witte, C. S.
 Yajnik, K. Yamamoto, T. Yamauchi, L. Yengo, K. Yoon, C. Yu, J.-M. Yuan, S. Yusuf,
 L. Zhang, W. Zheng, FinnGen, eMERGE Consortium, L. J. Raffel, M. Igase, E. Ipp,

- S. Redline, Y. S. Cho, L. Lind, M. A. Province, C. L. Hanis, P. A. Peyser, E. Ingelsson, A. B. Zonderman, B. M. Psaty, Y.-X. Wang, C. N. Rotimi, D. M. Becker, F. Matsuda, Y. Liu, E. Zeggini, M. Yokota, S. S. Rich, C. Kooperberg, J. S. Pankow, J. C. Engert, Y.-D. I. Chen, P. Froguel, J. G. Wilson, W. H. H. Sheu, S. L. R. Kardia, J.-Y. Wu, M. G. Hayes, R. C. W. Ma, T.-Y. Wong, L. Groop, D. O. Mook-Kanamori, G. R. Chandak, F. S. Collins, D. Bharadwaj, G. Paré, M. M. Sale, H. Ahsan, A. A. Motala, X.-O. Shu, K.-S. Park, J. W. Jukema, M. Cruz, R. McKean-Cowdin, H. Grallert, C.-Y. Cheng, E. P. Bottinger, A. Dehghan, E.-S. Tai, J. Dupuis, N. Kato, M. Laakso, A. Köttgen, W.-P. Koh, C. N. A. Palmer, S. Liu, G. Abecasis, J. S. Kooner, R. J. F. Loos, K. E. North, C. A. Haiman, J. C. Florez, D. Saleheen, T. Hansen, O. Pedersen, R. Mägi, C. Langenberg, N. J. Wareham, S. Maeda, T. Kadowaki, J. Lee, I. Y. Millwood, R. G. Walters, K. Stefansson, S. R. Myers, J. Ferrer, K. J. Gaulton, J. B. Meigs, K. L. Mohlke, A. L. Gloyn, D. W. Bowden, J. E. Below, J. C. Chambers, X. Sim, M. Boehnke, J. I. Rotter, M. I. McCarthy, and A. P. Morris (2022). Multi-ancestry genetic study of type 2 diabetes highlights the power of diverse populations for discovery and translation. *Nat. Genet.* 54(5), 560–572.
- Mbatchou, J., L. Barnard, J. Backman, A. Marcketta, J. A. Kosmicki, A. Ziyatdinov, C. Benner, C. O’Dushlaine, M. Barber, B. Boutkov, L. Habegger, M. Ferreira, A. Baras, J. Reid, G. Abecasis, E. Maxwell, and J. Marchini (2021). Computationally efficient whole-genome regression for quantitative and binary traits. *Nat. Genet.* 53(7), 1097–1103.
- Meinshausen, N. and J. Rice (2006). Estimating the proportion of false null hypotheses among a large number of independently tested hypotheses. *Ann. Statist.* 34(1), 373–393.
- Mikhaylova, A. V., C. P. McHugh, L. M. Polfus, L. M. Raffield, M. P. Boorgula, T. W. Blackwell, J. A. Brody, J. Broome, N. Chami, M.-H. Chen, M. P. Conomos, C. Cox, J. E. Curran, M. Daya, L. Ekunwe, D. C. Glahn, N. Heard-Costa, H. M. Highland, B. D. Hobbs, Y. Ilboudo, D. Jain, L. A. Lange, T. W. Miller-Fleming, N. Min, J.-Y. Moon, M. H. Preuss, J. Rosen, K. Ryan, A. V. Smith, Q. Sun, P. Surendran, P. S. de Vries, K. Walter, Z. Wang, M. Wheeler, L. R. Yanek, X. Zhong, G. R. Abecasis, L. Almasy, K. C. Barnes, T. H. Beaty, L. C. Becker, J. Blangero, E. Boerwinkle, A. S. Butterworth, S. Chavan,

- M. H. Cho, H. Choquet, A. Correa, N. Cox, D. L. DeMeo, N. Faraday, M. Fornage, R. E. Gerszten, L. Hou, A. D. Johnson, E. Jorgenson, R. Kaplan, C. Kooperberg, K. Kundu, C. A. Laurie, G. Lettre, J. P. Lewis, B. Li, Y. Li, D. M. Lloyd-Jones, R. J. F. Loos, A. Manichaikul, D. A. Meyers, B. D. Mitchell, A. C. Morrison, D. Ngo, D. A. Nickerson, S. Nongmaithem, K. E. North, J. R. O’Connell, V. E. Ortega, N. Pankratz, J. A. Perry, B. M. Psaty, S. S. Rich, N. Soranzo, J. I. Rotter, E. K. Silverman, N. L. Smith, H. Tang, R. P. Tracy, T. A. Thornton, R. S. Vasan, J. Zein, R. A. Mathias, NHLBI Trans-Omics for Precision Medicine (TOPMed) Consortium, A. P. Reiner, and P. L. Auer (2021). Whole-genome sequencing in diverse subjects identifies genetic correlates of leukocyte traits: The NHLBI TOPMed program. *Am. J. Hum. Genet.* 108(10), 1836–1851.
- Sarkar, S. K. (2006). False discovery and false nondiscovery rates in single-step multiple testing procedures. *The Annals of Statistics* 34(1), 394–415.
- Skol, A. D., L. J. Scott, G. R. Abecasis, and M. Boehnke (2006). Joint analysis is more efficient than replication-based analysis for two-stage genome-wide association studies. *Nat. Genet.* 38(2), 209–213.
- Sun, Q., M. Graff, B. Rowland, J. Wen, L. Huang, T. W. Miller-Fleming, J. Haessler, M. H. Preuss, J.-F. Chai, M. P. Lee, C. L. Avery, C.-Y. Cheng, N. Franceschini, X. Sim, N. J. Cox, C. Kooperberg, K. E. North, Y. Li, and L. M. Raffield (2022). Analyses of biomarker traits in diverse UK biobank participants identify associations missed by european-centric analysis strategies. *J. Hum. Genet.* 67(2), 87–93.
- Vuckovic, D., E. L. Bao, P. Akbari, C. A. Lareau, A. Mousas, T. Jiang, M.-H. Chen, L. M. Raffield, M. Tardaguila, J. E. Huffman, S. C. Ritchie, K. Megy, H. Ponstingl, C. J. Penkett, P. K. Albers, E. M. Wigdor, S. Sakaue, A. Moscati, R. Manansala, K. S. Lo, H. Qian, M. Akiyama, T. M. Bartz, Y. Ben-Shlomo, A. Beswick, J. Bork-Jensen, E. P. Bottinger, J. A. Brody, F. J. A. van Rooij, K. N. Chitrala, P. W. F. Wilson, H. Choquet, J. Danesh, E. Di Angelantonio, N. Dimou, J. Ding, P. Elliott, T. Esko, M. K. Evans, S. B. Felix, J. S. Floyd, L. Broer, N. Grarup, M. H. Guo, Q. Guo, A. Greinacher, J. Haessler, T. Hansen, J. M. M. Howson, W. Huang, E. Jorgenson, T. Kacprowski, M. Kähönen, Y. Kamatani,

M. Kanai, S. Karthikeyan, F. Koskeridis, L. A. Lange, T. Lehtimäki, A. Linneberg, Y. Liu, L.-P. Lyytikäinen, A. Manichaikul, K. Matsuda, K. L. Mohlke, N. Mononen, Y. Murakami, G. N. Nadkarni, K. Nikus, N. Pankratz, O. Pedersen, M. Preuss, B. M. Psaty, O. T. Raitakari, S. S. Rich, B. A. T. Rodriguez, J. D. Rosen, J. I. Rotter, P. Schubert, C. N. Spracklen, P. Surendran, H. Tang, J.-C. Tardif, M. Ghanbari, U. Völker, H. Völzke, N. A. Watkins, S. Weiss, VA Million Veteran Program, N. Cai, K. Kundu, S. B. Watt, K. Walter, A. B. Zonderman, K. Cho, Y. Li, R. J. F. Loos, J. C. Knight, M. Georges, O. Stegle, E. Evangelou, Y. Okada, D. J. Roberts, M. Inouye, A. D. Johnson, P. L. Auer, W. J. Astle, A. P. Reiner, A. S. Butterworth, W. H. Ouwehand, G. Lettre, V. G. Sankaran, and N. Soranzo (2020). The polygenic and monogenic basis of blood traits and diseases. *Cell* 182(5), 1214–1231.e11.

Westfall, P. H. and S. S. Young (1993). *Resampling-based multiple testing: Examples and methods for p-value adjustment*, Volume 279. John Wiley & Sons.

Zhao, B., T. Li, S. M. Smith, D. Xiong, X. Wang, Y. Yang, T. Luo, Z. Zhu, Y. Shan, N. Matoba, Q. Sun, Y. Yang, M. E. Hauberg, J. Bendl, J. F. Fullard, P. Roussos, W. Lin, Y. Li, J. L. Stein, and H. Zhu (2022). Common variants contribute to intrinsic human brain functional networks. *Nat. Genet.* 54(4), 508–517.